A Renewed Model of CNA Regulation Involving Its C-Terminal Regulatory Domain and CaM[†]

Hailong Wang, Yanwei Du, Benqiong Xiang, Weilin Lin, Xin Li, and Qun Wei*

Department of Biochemistry and Molecular Biology, Beijing Normal University, Beijing Key Laboratory, Beijing 100875, P.R. China

Received December 28, 2007; Revised Manuscript Received February 21, 2008

ABSTRACT: Calcineurin is composed of a catalytic subunit (CNA) and a regulatory subunit (CNB). CNA contains the catalytic domain and three regulatory domains: a CNB-binding domain (BBH), a C-terminal calmodulin-binding domain (CBD), and an autoinhibitory domain (AID). We constructed a series of mutants of CNA to explore the regulatory role of its C-terminal regulatory domain and CaM. We demonstrated a more precise mechanism of CNA regulation by C-terminal residues 389–511 in the presence of CNB. First, we showed that residues 389–413, which were identified in previous work as constituting a CaM binding domain (CBD), also have an autoinhibiting function. We also found that residues 389–413 were not sufficient for CaM binding and that the CBD comprises at least residues 389−456. In conclusion, two distinct segments of the C-terminal regulatory region (389–511) of CNA inhibit enzyme activity: residues 389–413 interact with the CNB binding helix (BBH), and residues 457–482 with the active center of CNA.

Calcineurin (CN), a Ca^{2+}/calmodulin-dependent phosphatase, is the principal mediator of cellular responses triggered by intracellular Ca^{2+} signals. CN is ubiquitously expressed in human tissues, with the highest level in brain and the immune system. The protein functions mainly by regulating protein dephosphorylation. Abnormal levels of calcineurin in the cell cause many diseases, such as Alzheimer's disease, cardiac hypertrophy, and lesions of the immune system (*1–3*).

CN is a heterodimer composed of two subunits: a catalytic A-subunit (CNA) of 59 KD, and a regulatory B-subunit (CNB) of 19 KD. The CNB subunit is an "EF-hand" Ca^{2+}-binding protein that remains tightly associated with the A subunit in the presence or absence of Ca^{2+}. Ca^{2+} binding to the B subunit stimulates CN phosphatase activity, but this activity is low compared with that attained in the presence of Ca^{2+}/CaM (*2, 4*). CaM increases V_{max} whereas CNB primarily decreases the K_m with a smaller effect on V_{max} (*5*).

Mapping of CNA by limited proteolysis and structural analysis has revealed three regulatory domains: the CNB-binding domain (BBH, 350–370), a CaM-binding domain (CBD, 389–413) and an autoinhibitory domain (AID, 457–482) (*6–8*). Removal of residues 457–482 does not result in full Ca^{2+}/CaM-independent activity; instead full activity in the absence of Ca^{2+} requires the removal of residues 420–457. Truncation of the C-terminal of CNA indicated the presence of several autoinhibitory motifs as well as an additional autoinhibitory element within residues 420–457 (*5, 9*). The crystal structure of CN revealed that the AID (457–482) interacts with the catalytic core, providing direct evidence for its autoinhibitory function (*7*). However, to date, most of the C-terminal region of CNA apart from the AID (457–482) is missing from the published structures. How the other autoinhibitory elements in this region exert their autoinhibitory effects remains unknown.

As with many CaM-regulated enzymes, CN autoinhibition is controlled by CaM binding. CaM, an EF-hand protein, binds to Ca^{2+}, and this enables it to bind to the CBD of CNA and expose the CN active site. CaM is a ubiquitous intracellular Ca^{2+}-sensor that plays an important role in several downstream GPCR signaling pathways (*10, 11*). It can bind to and modulate a diverse array of cellular proteins, including enzymes, ion channels, transcription factors, and cytoskeletal proteins (*12, 13*). The presence of the CaM-binding region in CNA has been inferred from the fact that the consensus structure and sequence of this region is highly related to other CaM-regulated protein sequences (*14*). The CBD precedes the AID domain in CNA, unlike what is found in CaM-dependent protein kinases (CaMKK and CaMKII) as well as myosin light chain kinase (MLCK), where the CaM binding regions generally follow or partially overlap with the autoinhibitory domains in the primary sequences (*15–17*). To date, there is no detailed experimental evidence indicating how CaM binds to and regulates CN.

In this report we describe truncation and site mutagenesis studies that lead us to propose a two-site inhibitory model. In addition we examined the binding of CaM to CNA by pull-down and SPR experiments. The results reveal a new organization of the functional domains of CNA involving a more precise mechanism of CNA regulation by the C-terminal regulatory segments and CaM.

[†] This work was supported by grants from the National Science Foundation of China, the Research Fund for the Doctoral Program of Higher Education, the National Important Basic Research Project, and the Guangdong Province-Education Ministry Combined Fund.

* Corresponding author. Tel: +86-10-58807365. Fax: +86-10-58807365. E-mail: weiq@bnu.edu.cn.

10.1021/bi702539e CCC: $40.75
Published on Web 03/19/2008

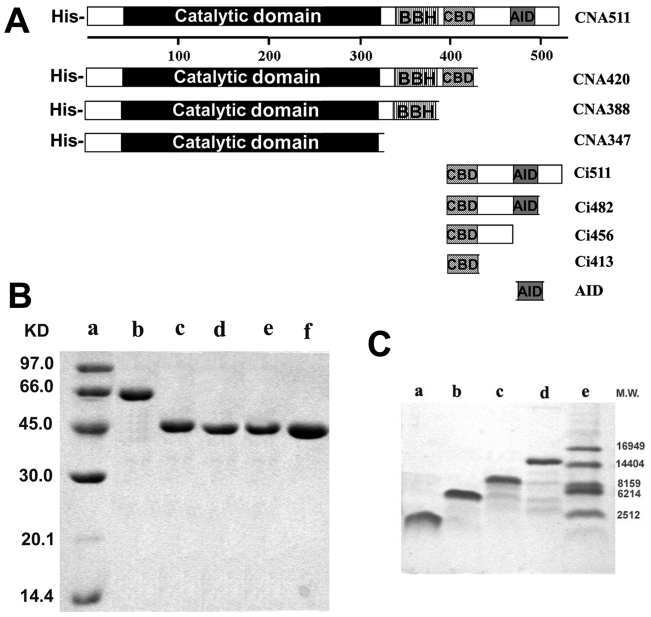

FIGURE 1: (A) Schematic representation of CNA and its domain deletion mutants. The abbreviations used are as follows: CNA511, wild type CNA containing the full-length calcineurin A subunit; CNA420, CNA deleted from residue 420, containing residues 1–420; CNA388, CNA deleted from residue 388, containing residues 1–388; CNA347, CNA truncated deleted from residue 347, containing residues 1–347. Ci511, the full-length C-terminal regulatory segment containing residues 389–511; Ci482 containing residues 389–482; Ci456 containing residues 389–456; Ci413 containing residues 389–413; the classical autoinhibitory domain AID containing residues 457–482. (B) SDS−PAGE analysis of the purified proteins. [The proteins were run on a 14% acrylamide gel and stained with Coomassie Blue. (a) Markers; (b) CNA511; (c) CNA420; (d) CNA388; (e) CNA388E/Q; (f) CNA347.] (C) Tricine-SDS−PAGE analysis of purified C-terminal segments of CNA [(a) Ci413; (b) Ci456; (c) Ci482; (d) Ci511; (e) markers].

MATERIALS AND METHODS

Materials. The *Escherichia coli* strains BL21 (DE3), DH5α, the expression vector pET-21a (+), pET-28a (+), the rat CNA-α cDNA clone, CaM-Sepharose, purified CNB and CaM proteins were from our laboratory collection. RII peptide was purchased from BioMol Research Laboratories Inc., and the AID peptide was synthesized and purified by New England BioLabs. PPO[$OC(C_6H_5)$═NCH═CC_6H_5] and POPOP{[$OC(C_6H_5)$═CHN═$C]_2C_6H_4$} were obtained from the E. Merck Corp. [γ-^{32}P]-ATP was from Beijing Furi Biology Engineering Corp, and cAMP dependent protein kinase catalytic subunit was from Promega Chemical Corp. Restriction enzymes (*Nde*I and *Bam*HI), T4 DNA ligase, and Pyrobest polymerase were purchased from TaKaRa Biotech (Tokyo, Japan), and thrombin was from Sigma Corp. Protein standard, DEAE Sepharose FF, SP Sepharose, HisTrap HP, and Sephacryl S200 HR were purchased from Amersham Biosciences. All other reagents were of standard laboratory grade and of the highest quality available from commercial suppliers.

Cloning, Protein Expression and Purification of CNA and Its C-Terminal Deletion Mutants. The domain map of CNA is shown in Figure 1A. The expression vectors pET28a/CNA511, pET28a/CNA420, pET28a/CNA388, and pET28a/CNA347 were constructed using the *Nde*I and *Hin*dIII restriction sites in the CNA-α cDNA template using standard PCR and molecular cloning methods. The complete sequences of all constructs were confirmed by DNA sequencing. The constructed expression vectors were transformed into BL21 (λDE3), grown in LB medium at 37 °C (with 1‰ w/v ampicillin) and then expressed at 25 °C overnight, in the presence of 50 μM IPTG. For CNA511, purification was carried out as previously described except that after CaM-Sepharose, an additional step of immobilized metal affinity chromatography was included (*18, 19*). In brief, after the desired proteins were eluted from CaM-Sepharose column, the active fractions were diluted with binding buffer (20 mM Mops, 40 mM imidazole, 0.5 M NaCl), applied to a His-Trap column, and eluted with a linear gradient of elution buffer (20 mM Mops, 500 mM imidazole, 0.5 M NaCl). For the three deletion mutants, purification was also carried out as previously described, but the DEAE-column was replaced by a His-Trap column; the active fractions from the Sephacryl- S200 HR column were dealt with by the same method as for CNA511 (*20, 21*). Protein purity was assessed by SDS−PAGE, and protein concentrations were measured by the procedure of Bradford (*22*).

Cloning, Protein Expression and Purification of the C-Terminal Segments of CNA. Previously, we reported a three-step PCR procedure for creating the fusion protein CcL (CBD of CNA fused to the C-terminus of CaM via a 5-glycine flexible linker) (*23*). In this work, the pET21a-CciT511 plasmid, which contains a continuous DNA sequence coding for CaM, a thrombin cleavage site, and the C-terminus of CNA (CNA389–511), was constructed by the same method. In addition, fusion vector pET21a-CciT482 (containing CaM, a thrombin cleavage site, and CNA389-482), pET21a-CciT456 (containing CaM, a thrombin cleavage site, and CNA389-456) and pET21a-CciT413 (containing CaM, a thrombin cleavage site, and CNA389-413) were constructed from the pET21a-CciT511 template by standard PCR and molecular cloning methods. The complete sequences of all the constructs were confirmed by DNA sequencing, and the constructs were transformed into BL21 (λDE3). The fusion proteins CciT511, CciT482, CciT456, and CciT413 were expressed and purified by the same method as CcL. The CaM tag was cleaved off by digesting with recombinant thrombin, in a ratio of 1 mg of CaM-CBD to 1 unit of thrombin, at 25 °C for 24 h, and the thrombin was inactivated by heating the reaction mixture to 85 °C for 25 min. After centrifugation for 30 min at 20 000 rpm, EGTA was added to the supernatant to a final concentration of 5 mM and the suspension incubated for 30 min at room temperature. It was then diluted with buffer C (20 mM Tris-HCl pH 7.6, 5 mM EGTA, 0.2 mM PMSF, 0.1% β-mercaptoethanol) and loaded onto a dual column of DEAE (Pharmacia) anion-exchanger and SP (Pharmacia) cation-exchanger columns connected in-line and pre-equilibrated with buffer C. The C-terminal peptide did not bind to DEAE and was washed down to the SP column with buffer C. The DEAE column was then removed, and the peptides bound to the SP column were eluted with a linear salt gradient from buffer C to B (20 mM Tris-HCl pH 7.6, 5 mM EGTA, 0.2 mM PMSF, 0.1% β-mercaptoethanol, 1 M NaCl). The peak fractions were loaded on a G-25 column to remove the salt, eluted with Milii-Q water, lyophilized and stored at −30 °C until further use.

Assay of Phosphatase Activity. Phosphatase activity was assayed as described (*21*). All purified enzymes were

concentrated with an Amicon Ultra Filter Unit and diluted more than 500-fold for assays. Ten microliters of diluted enzyme solution (50 mM Tris-HCl, pH 7.4, 0.1 mg/mL BSA, 0.5 mM DTT and 1 mM Mn^{2+}, 0.2 mM $CaCl_2$, 0.6 μM CaM and 0.6 μM CNB) was mixed with 10 μL of assay buffer (60 μM ^{32}P-labeled RII peptide, 50 mM Tris-HCl, 0.5 mM DTT, 0.1 mg/ml BSA), and reactions were performed at 30 °C for 10 min, and terminated by adding 0.18 mL of 83.3 mM H_3PO_4. Finally, the released ^{32}Pi was separated from RII peptide and quantified by liquid scintillation spectrometry. Units of activity were defined as nanomoles of ^{32}Pi released from RII peptide per minute. Various concentrations of ^{32}P-labeled RII peptide were used for measuring the kinetic properties of CNA and its derivatives.

Inhibition of Phosphatase Activity by Autoinhibitory Segments. In order to assay the inhibition of phosphatase activity of CNA by its C-terminal autoinhibitory segments, the enzyme was diluted to 20 nM in dilution buffer (50 mM Tris-HCl, pH 7.4, 0.1 mg/ml BSA, 0.5 mM DTT and 1 mM Mn^{2+}, 0.2 mM $CaCl_2$, 0.6 μM CNB). The various C-terminal peptides were also diluted to different concentrations in the same buffer. The diluted inhibitory peptides and enzyme were mixed 1:1 (v:v) and incubated on ice for 10 min. Ten microliters of each mixture was then added to 10 microliters of assay buffer (60 μM ^{32}P-labeled RII peptide, 50 mM Tris-HCl, 0.5 mM DTT, 0.1 mg/ml BSA) to initiate the phosphatase assay.

Kinetic Analysis of Ci413 and AID Peptide. For kinetic analysis, the concentration of ^{32}P-labeled RII peptide was varied from 2.5 μM to 80 μM for each concentration of a given autoinhibitory segment. The autoinhibitory segments were assayed at three concentrations: 0 μM, 3.9 μM and 15.6 μM, and the data were fitted to nonlinear regression equations. Lineweaver–Burke plots were generated by linear-regression analysis of the data.

Analysis of Electrostatic Potentials. The electrostatic potentials of CNA388 and Ci413, AID in pH7.4 buffer were calculated by the finite difference Poisson–Boltzmann method (Delphi program in Insight II). PDB: 1AUI and 2F2O were calculated (*23, 24*). AID and Ci413 were unmerged from the respective complexes. The solvent-accessible surface was mapped with different colors according to the calculated electrostatic potential energy values.

Site-Directed Mutation. The two-round PCR method was used to construct the amino acid substitution mutants. *Nde*I and *Hin*dIII restriction sites were introduced at the 5′- and 3′-ends of the primers, respectively, and the PCR products were subcloned into the pET-21a expression vector using these restriction sites. DNA was sequenced by the dideoxynucleotide method.

Pull-Down Assays. The expression vectors pET21a/CNA511, pET21a/CNA456, pET21a/CNA420, and pET21a/CNA347 in BL21 (λDE3) were expressed as described (*21*), and the cell pellet from 500 mL of *E. coli* culture was resuspended in 15 mL of lysis buffer (50 mM Tris, pH 7.4, 1 mM EDTA, 0.2 mM PMSF and 20 mM β-mercaptoethanol) and lysed by sonication. The lysate was clarified by centrifugation at 40000*g* for 20 min, and to the supernatant was added 2 mM $CaCl_2$, and then 100 μL of equilibrated CaM-Sepharose was added to 1.5 mL of the soluble extract. The mixture was incubated for 2 h at 4 °C, with gentle mixing. After washing the beads three times with 1 mL of equilibrated buffer (50 mM Tris, pH7.4, 2 mM $CaCl_2$, 0.2 mM PMSF and 20 mM β-mercaptoethanol) bound protein was eluted with 2 × SDS loading buffer. Aliquots were loaded onto an SDS−PAGE gel, transferred to a nitrocellulose membranes, and the proteins detected by Western blotting.

Surface Plasmon Resonance. Real-time binding and kinetic analyses were performed at the Institute of Biophysics, Chinese Academy of Sciences, on a BIAcore 3000 biosensor system (Pharmacia Biosensor AB) using surface plasmon resonance (SPR) measurements. Carboxymethylated sensor chips (type CM5) were activated with a 1:1 mixture of 0.2 M *N*-ethyl-*N*′-(3-dimethylaminopropyl) carbodiimide and 0.05 M *N*-hydroxy-succinimide in water. C-Terminal peptides of CNA were then immobilized on the sensor chips using an amine coupling kit (BIAcore) as described by the supplier. Unreacted sites were blocked with 1 M ethanolamine (pH 8.5). Control flow cells were activated and blocked in the absence of protein. Binding was evaluated over a range of CaM concentrations in 150 mM NaCl, 100 mM HEPES (pH 7.4), and 500 mM $CaCl_2$ under a continuous flow of 30 μ/min at 25 °C. CaM-containing solution (90 μL) was pulsed over the surface of the chip for 3 min using the kinject command. Binding of CaM to flow cell-immobilized peptide was corrected for binding to control flow cells. Flow cells were regenerated by passing over running buffer with 2 mM EGTA. Binding data were calculated using BIAevaluation software version 4.1.

RESULTS

Expression and Purification of Proteins. CNA and its derivates were purified (see Materials and Methods) and analyzed by SDS−PAGE. All the proteins were electrophoretically pure (Figure 1B). The purified C-terminal segments of CNA were analyzed by Tricine-SDS−PAGE. As shown in Figure 1C, electrophoretically pure peptides were obtained.

Inhibition of Phosphatase Activity by Ci Segments. In order to explore the mechanism of CNA inhibition by its C-terminal regulatory domains, various C-terminal regulatory segments containing different C-terminal region were expressed and purified by the CaM-fusion method. The deletion mutants CNA388 and CNA347 of CNA were used to assay inhibition of phosphatase activity because both lack the entire C-terminal regulatory domain and can function only in catalysis. Phosphatase activity was examined in titration experiments using multiple concentrations of peptides and ^{32}P-labeled RII peptide as substrate. As shown in the dose response curves of Figure 2A and Table 2, the phosphatase activity of CNA388 was inhibited by all the C-terminal segments. The complete C-terminal region of CNA, designated Ci511, was the most inhibitory, with an IC_{50} of 30 nM. The order of inhibition was Ci511 > Ci482 > Ci456, Ci413 > AID. It is interesting that Ci413, which was considered a CaM binding domain (CBD) in previous work, also inhibited CNA388 and was more effective as an inhibitor than the classical autoinhibitory peptide (AID). CNA347 differs from CNA388, in that the BBH is also deleted. This protein was also used in inhibition experiments, and it can be seen from Figure 2B and Table 2 that all the peptides except AID were less inhibitory for CNA347 than for

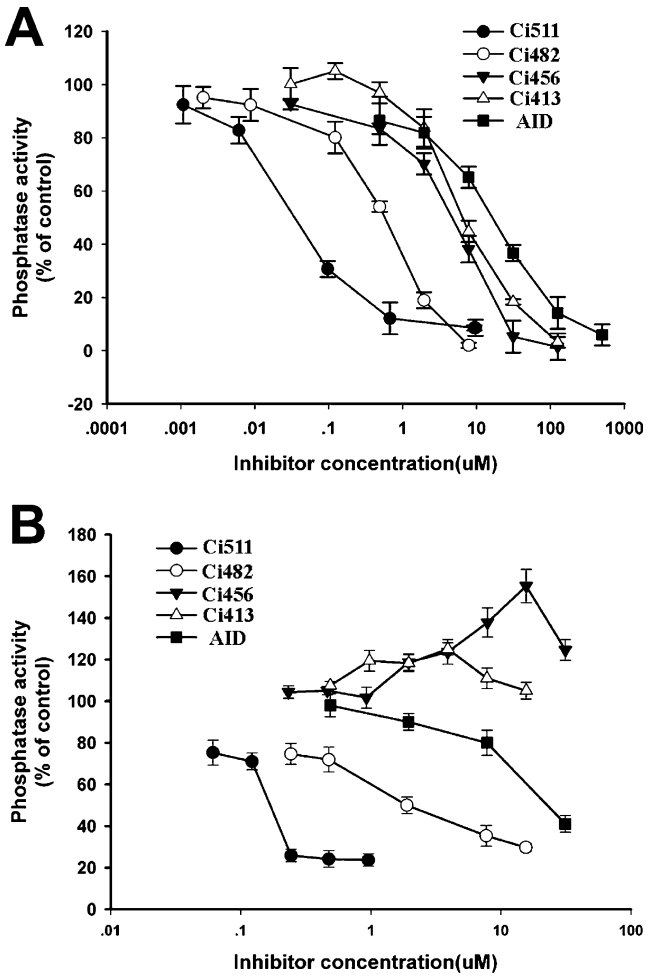

FIGURE 2: Inhibition of phosphatase activity by various C-terminal segments. (A) Inhibition of CNA388 by the Ci segments. The final concentration of CNA388 was 5 nM. CNB was present, and CaM was absent from the assay system. (B) Inhibition of CNA347 by the Ci segments. The final concentration of CNA347 was 5 nM. CNB was present, and CaM was absent from the assay system. All data are expressed as mean ± SD of the phosphatase activity in three separate experiments.

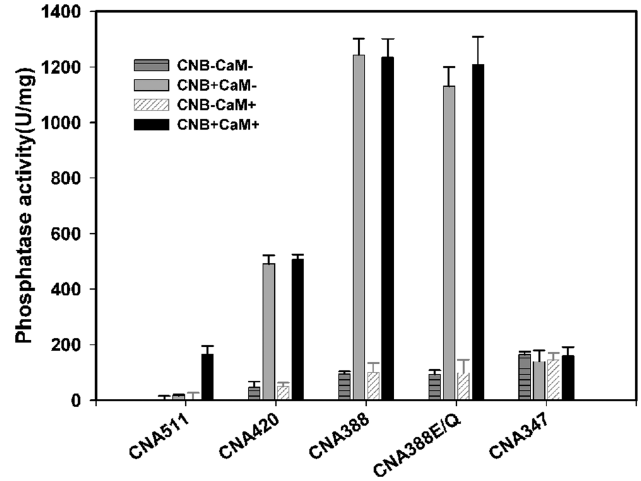

FIGURE 3: Phosphatase activities of CNA511 and its derivatives (30 μM ^{32}P-RII as substrate, see the Materials and Methods section. All data are expressed as mean ± SD of the phosphatase activity in three separate experiments).

Table 1: Enzyme Kinetics of CNA and Its Derivatives[a]

	CNA511	CNA420	CNA388	CNA347
V_{max} (U/mg)	12 ± 1	833 ± 34	4000 ± 58	557 ± 21
K_m (μM)	26 ± 2	64 ± 3	45 ± 3	60 ± 4
K_{cat} (s^{-1})	0.01 ± 0.00	0.66 ± 0.03	12.89 ± 0.40	0.41 ± 0.03

[a] All data are expressed as mean ± SD. The mean enzyme kinetics parameters from at least three independent sets of kinetic experiments are reported. CNB was present, and CaM was absent from the assay system.

Table 2: IC_{50} Values of CNA388 and CNA347 for Ci Segments[a]

	Ci511 (μM)	Ci482 (μM)	Ci456 (μM)	Ci413 (μM)	AID (μM)
CNA388	0.03 ± 0.01	0.58 ± 0.03	4.92 ± 0.20	6.63 ± 0.18	17.06 ± 0.65
CNA347	0.13 ± 0.01	1.82 ± 0.09			13.85 ± 0.66

[a] All data are expressed as mean ± SD of the IC_{50} values in three separate experiments. The final concentrations of CNA388 and CNA347 were 5 nM. CNB was present, and CaM was absent from the assay system.

CNA388. In addition, unlike CNA388, CNA347 was not inhibited by Ci413 and Ci456, which do not contain the AID region.

Phosphatase Activities of CNA and Its Derivatives. We assayed the phosphatase activities of CNA and its derivatives with ^{32}P-labeled RII peptide as substrate, as described. In the presence of CNB and absence of CaM, the order of activity was CNA388 > CNA420 > CNA511, CNA347 (Figure 3). The enzymatic parameters of wt CNA and its derivatives are shown in Table 1. Deletion of residues 389–413 of CNA also resulted in an increase of V_{max}. CNA388 had a higher V_{max} than CNA420 and the other mutants. In addition, the phosphatase activity of CNA420 could not been enhanced by CaM although this protein retained the CBD (389–413) (Figure 3).

Kinetic Mechanism of CNA388 Inhibition by Ci413 and AID Peptides. The results above indicated that residues 389–413 of the C-terminus of CNA, which were considered a CaM binding domain (CBD), are also autoinhibitory. To explore the basis of this autoinhibitory effect we examined the kinetics of phosphatase inhibition by Ci413 and compared it with the classical autoinhibitory peptide AID. As shown in Figure 4, the kinetics were studied by measuring CN388 phosphatase activity at various ^{32}P-RII peptide concentrations, in the presence or absence of 3.9 or 15.6 μM inhibitory peptide. The reciprocal plot indicated that inhibition of phosphatase activity by AID with ^{32}P-RII peptide as substrate was competitive whereas Ci413 proved to be a noncompetitive inhibitor.

Mutations in the BBH Decrease the Inhibition of CNA388 by Ci413. Evidently Ci413 and AID inhibit phosphatase activity by different mechanisms. The crystal structure of CN shows that AID inhibits phosphotase activity by covering the active site. We were therefore interested to identify the binding site for Ci413 on the enzyme. By analyzing basic biochemical properties we found that the theoretical PIs of Ci413 and AID were very different: 12.01 for Ci413 compared with 6.28 for AID. This difference suggested a role for electrostatic attraction in the interaction between the inhibitors and the enzyme. In previous work we isolated a complex of CaM and CBD (CNA residues 389–413; designated Ci413 here). Up to now, this provided the only structural information about the CBD of CNA. That complex and a part of the CNA/CNB complex (PDB: 1AUI) were used to calculate the solvent accessible surfaces and elec-

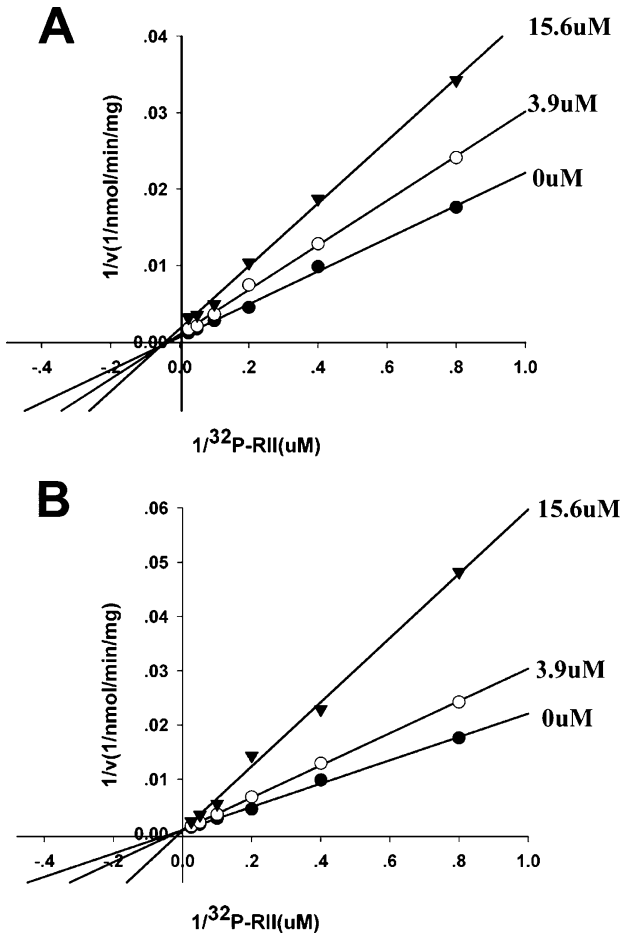

FIGURE 4: Kinetic analysis of the inhibitory mechanism of Ci413 (A) and AID (B). CNA388 activity was determined in the presence of CNB and zero, 3.9 μM or 15.6 μM inhibitor (Ci413 or AID).

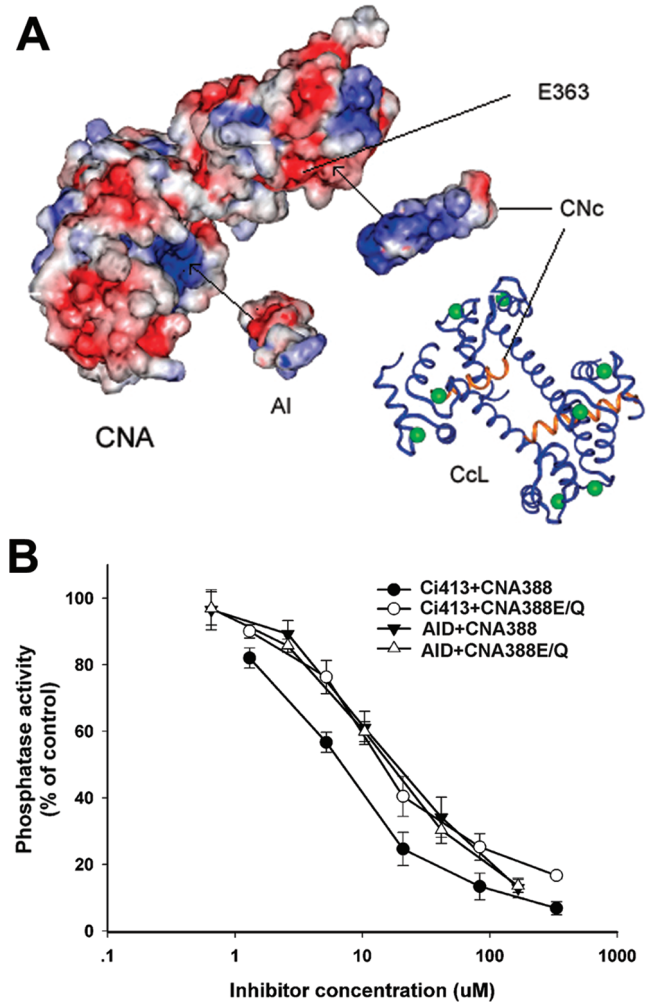

FIGURE 5: (A) Electrostatic potentials of CNA388, Ci413 and AID in pH7.4 buffer (PDB: 1AUI and 2F2O were used to calculate). The solvent accessible surface is mapped with different colors according to the calculated electrostatic potential energy values: positive charge, blue; neutral, white; negative charge, red. (B) Inhibition of CNA388 and CNA388E/Q by Ci413 and AID. CNA388E/Q is a site-directed mutant of CNA388, in which Glu residues 359 and 363 were mutated to Gln. The final concentrations of the enzymes were 5 nM. CNB was present, and CaM was absent from the assay system.

trostatic potential distributions on the surfaces by the methods described in the previous section. From Figure 5A, it is easy to see that the positive electrostatic potential areas on the surface of Ci413 are much larger than the negative ones. In contrast, the surface of the AID shows the reverse electrostatic potential, with larger negative electrostatic potential areas on its surface. In addition, there are obvious positive areas on the active site of the catalytic domain which could be responsible for binding the AID. In other words, the active site on the enzyme does not appear to be the binding site for Ci413. Moreover, we located an obvious negative region on the surface of the CNB/BBH complex (Figure 5A). As the two acidic residues Glu359 and Glu363 of the BBH are located on this surface, we mutated them to Gln, yielding the mutant form designated CNA388E/Q, to test if mutations on the BBH of CNA affect the inhibition by inhibitors. The results in Figure 5B show that CNA388E/Q is less sensitive to Ci413 than wt CNA388 but has the same sensitivity to the AID peptide.

Binding of CNA and Its Derivatives to CaM-Sepharose. As shown in Figure 3, CNA420 was not activated by CaM although it includes the presumed CBD (389–413). We have presented evidence that the CBD (Ci413, 389–413 of CNA) has a new inhibitory function. This raises the question of why the inhibition of CNA420 by CBD cannot be reversed by CaM as it can be in wt CNA and the other mutants. Actually, we found that CNA420 could also not be purified by CaM-Sepharose. This implies that the binding between CaM and CNA420 is weak. We carried out a CaM-Sepharose pull-down experiment to assay binding of CaM with wt-CNA and its deletion mutants. As shown in Figure 6B, both in the presence and in the absence of CNB, CaM pulled down wt-CNA, CNA482, and CNA456 whereas CNA420 and the control CNA347 were not pulled down. These results confirm the idea that CaM does not bind efficiently to CNA420. Hence we conclude that the CBD in CNA does not mediate strong binding between CNA and CaM.

Interactions of CaM with Ci Segments. The interactions between CaM and a series of C-terminal segments of CNA were further examined by SPR using BIAcore 3000 sensor technology. As shown in Figure 7, CaM rapidly and reversibly interacted with the C-terminal segments in the presence of Ca^{2+}, but not in the presence of EGTA, and showed typical saturation behavior. The kinetic and equilibrium affinity parameters of the interactions of the Ci segments with CaM are presented in Table 3. Ci413 obviously differs from the other peptides both in the kinetics of the interaction and in competence to bind to CaM. We

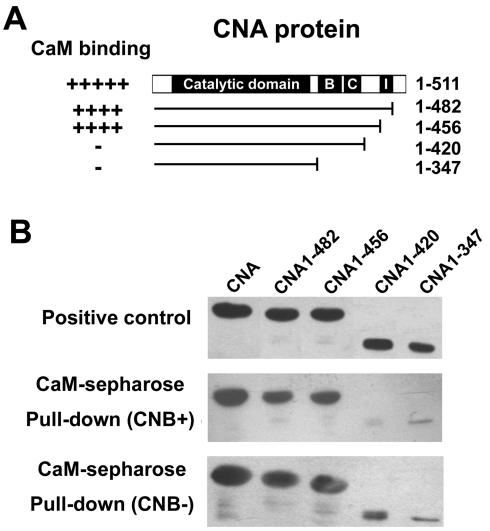

FIGURE 6: CaM binding properties of CNA and its derivatives.

were unable to calculate the association or dissociation rate constant of Ci413 with CaM, in part due to the very high on/off rates, which were beyond the limits of the software. However, the kinetics of the interactions of the other three peptides Ci511, Ci482 and Ci456 with CaM were similar, with similar association and dissociation rate constants. In addition, we obtained a K_D value of 78.9 nM for the Ci413−CaM interaction, 100-fold higher than for the other peptides. These results are consistent with our CaM-Sepharose pull-down studies in showing that the affinity of Ci413 for CaM is much lower than that of the other peptides.

DISCUSSION

In our previous work, we used a CaM-fusion method to obtain purified C-terminal segments of CNA (*24*). The main purpose of that work was to determine the structure of the C-terminal domain of CNA which was missing from all published structures of CN. In the present work we focused on the function of this region. We obtained a series of C-terminal segments of CNA containing different regulatory regions by the CaM-fusion method. These purified peptides facilitated examination of their regulatory role and binding to CaM.

New Function of Residues 389–413 of CNA. Previous work using overlapping synthetic peptides identified an autoinhibitory element within residues 457−482 of CNA (*8*). However, removal of this region resulted in phosphatase activity that was only partially Ca^{2+}/CaM-independent. Further work indicated the presence of additional autoinhibitory element(s) within residues 420–457 of CNA (*5, 9*). In addition, many workers have proposed that residues 389–413 of CNA are responsible for CaM binding (*1, 25*). However

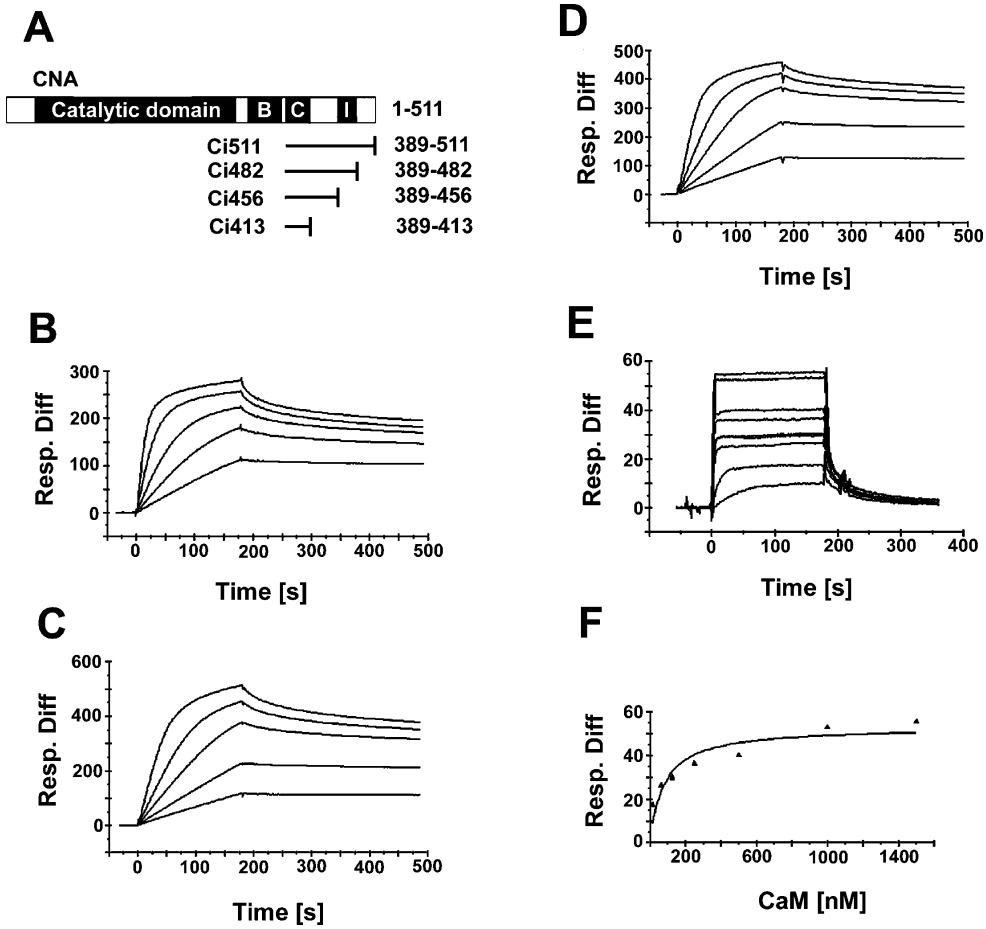

FIGURE 7: SPR analysis of the interactions of the Ci segments with CaM. (B−D) Sensorgrams were recorded with Ci511(B), Ci482 (C), Ci456 (D) immobilized on a CM5 sensor chip and CaM (3.9, 7.8, 15.6, 31.25 and 62.5 nM) using a BIAcore 3000 biosensor. Kinetic data for the three peptides fitted a 1:1 Langmuir model. (E). Sensorgrams were recorded with immobilized Ci413 peptide and CaM (3.9, 15.6, 62.5, 125, 250, 500 nM and 1, 1.5 μM) using a BIAcore 3000 biosensor. The kinetic data with this peptide did not fit a 1:1 Langmuir model and were instead evaluated using steady-state analysis in which the equilibrium responses (R_{eq}) were plotted against CaM concentration (F).

this region was assigned a CaM binding role despite the fact that its accurate location was not known. In this work, we identified an inhibitory effect of the classical CaM binding domain. We showed in particular that residues 389–413 of CNA contribute to both CaM binding and autoinhibition. In other words, this region has a dual function.

Two Sites Inhibitory Model of CNA by Its C-Terminal Regulatory Domain. The crystal structure indicated that the classical autoinhibitory peptide 457–482 interacts with the active center to inhibit phospatase activity (*7*). However, Ci413 was absent from all published structures, and there were no reports concerning its possible inhibitory function. We found that unlike the AID, Ci413 inhibited the phosphatase activity of CNA388 but did not inhibit the phosphatase activity of CNA347. CNA347 contains an intact catalytic domain but lacks the BBH. This implied that the BBH was necessary for inhibition by Ci413 but not by the AID. We examined the kinetic mechanism of CNA388 inhibition by Ci413 and compared it with the classical autoinhibitory peptide AID. As shown in Figure 4, the kinetics of CNA388 inhibition by Ci413 also differed from that of the AID peptide. AID exhibited competitive inhibition whereas Ci413 was a noncompetitive inhibitor, suggesting that it does not inhibit by interacting with the active site of the enzyme. This raises the question of how Ci413 affects the phosphatase activity of the enzyme. As shown in Figure 5B, mutations in the BBH of CNA affected the inhibitory potencies of Ci413 whereas inhibition by the AID was not affected by such mutations. It is thus clear that Ci413 inhibits phosphatase activity by interacting with the BBH, and that the C-terminal regulatory segments of CNA inhibit enzyme activity by different mechanisms. The main role of the BBH is to mediate regulation of CNA by CNB (*1, 25*). Some reports also suggest that it is also a binding site for substrate (*26, 27*). In addition, the crystal structure and many experiments indicate that the composite surface formed by BBH of CNA and CNB is the common binding site for the two immunophilin–immunosuppressant complexes Cyp−CsA and FKBP−FK506 (*28–31*). Ci413 binding to BBH could inhibit the phosphatase activity by altering the interaction of CNA with CNB or affecting substrate binding.

Binding of CaM with CNA. As previously described, CNA autoinhibition is controlled by CaM binding. However, the presumptive CaM-binding region of CN precedes the AID domain, unlike what is found in other CaM-regulated enzymes. Actually, until now there was no detailed experimental evidence about which regions in CNA are responsible for CaM binding. This made it difficult to clarify the mechanism by which CNA activity is regulated by CaM and to obtain the complex structure of CaM with CNA or with peptides of CNA. Our present results indicate that the CBD (389–413) of CNA identified in previous work is not sufficient for CaM binding (Figures 6, 7). The newly defined CaM-binding functional domain resembles the situation in some other CaM-regulated proteins in which the CBD partially overlaps with an autoinhibitory domain in the primary sequence.

New Functional Domain Organization of CNA. As shown in Figure 8A, in the domain organization of CNA as it appears at present, the CaM binding domain precedes the autoinhibitory domain near the carboxyl terminus of CNA. As shown in Figure 8B,C, we propose that the entire C-terminal of CNA (389–511) is included in the "NEWAID" domain, which inhibits phosphatase activity by two mechanisms. Residues 389–413 bind to BBH, and residues 457–482 bind to the active site. In addition, the "NEWCBD" domain, which is responsible for CaM binding to CNA, is included in the "NEWAID" domain, and comprises residues 389–456. The classical CBD domain is not sufficient for binding with CaM (Figures 6, 7): residues 413–456 affect both the affinity and dynamics of the binding of CNA (or its peptides) with CaM.

Table 3: Summary of the Kinetic and Equilibrium Affinity Parameters of the Ci Segments−CaM Interactions[a]

	k_a (10^6 M^{-1} s^{-1})	k_d (10^{-4} s^{-1})	K_A (10^9 M^{-1})	K_D (10^{-10} M)	model
Ci511	1.05 ± 0.01	7.30 ± 0.05	1.44 ± 0.13	6.93 ± 0.29	1:1 binding
Ci482	1.10 ± 0.01	9.79 ± 0.19	1.12 ± 0.25	8.91 ± 0.33	1:1 binding
Ci456	1.17 ± 0.03	5.73 ± 0.09	2.04 ± 0.33	4.91 ± 0.41	1:1 binding
Ci413			1.27 ± 0.08	7.89 ± 0.49	steady state affinity

[a] The mean binding parameters from at least three independent sets of kinetic experiments are reported. Errors represent standard deviations of the experimental values derived from independent kinetic measurements.

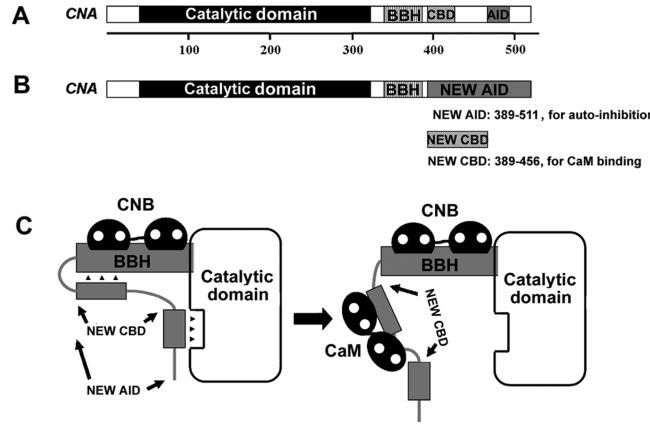

FIGURE 8: Schematic representation of the regulation of CNA activity by its C-terminal regulatory domain and CaM. (A) The previous model of the domain organization of CNA. (B) The new model. Entire C-terminal of CNA (389–511) is included in the "NEWAID" domain and the "NEWCBD" domain is included in the "NEWAID" domain, and comprises residues 389–456. The presumptive CaM-binding region in previous works is not enough for CaM binding. (C) Two-site inhibition model of CNA by its C-terminal regulatory domain and CaM. Residues 389–413 interact with the CNB binding helix (BBH), and residues 457–482 with the active center of CNA to inhibit activity of the enzyme.

ACKNOWLEDGMENT

We thank Dr. Yuanyuan Chen for help with the SPR assays.

REFERENCES

1. Rusnak, F., and Mertz, P. (2000) Calcineurin: form and function. *Physiol. Rev. 80*, 1483–1521.
2. Klee, C. B., Ren, H., and Wang, X. T. (1998) Regulation of the calmodulin-stimulated protein phosphatase, calcineurin. *J. Biol. Chem. 273*, 13367–13370.
3. Aramburu, J., Rao, A., and Klee, C. B. (2000) Calcineurin: from structure to function. *Curr. Top. Cell. Regul. 36*, 237–295.
4. Klee, C. B., Draetta, G. F., and Hubbard, M. J. (1988) Calcineurin. *Adv. Enzymol. Relat. Areas Mol. Biol. 61*, 149–200.

5. Perrino, B. A., Ng, L. Y., and Soderling, T. R. (1995) Calcium regulation of calcineurin phosphatase activity by its B subunit and calmodulin. *J. Biol.Chem. 270*, 340–346.
6. Hubbardt, M. J., and Klee, C. B. (1989) Functional Domain Structure of Calcineurin A: Mapping by Limited Proteolysis. *Biochemistry 28*, 1868–1874.
7. Kissinger, C. R., Parge, H. E., Knighton, D. R., Lewis, C. T., Pelletier, L. A., Tempczyk, A., Kalish, V. J., Tucker, K. D., Showalter, R. E., and Moomaw, E. W. (1995) Crystal structures of human calcineurin and the human FKBP12-FK506-calcineurin complex. *Nature 378*, 641–644.
8. Hashimoto, Y., Perrino, B. A., and Soderling, T. R. (1990) Identification of an autoinhibitory domain in calcineurin. *J. Biol. Chem. 265*, 1924–1927.
9. Perrino, B. A. (1999) Regulation of CN phosphatase activity by its autoinhibitory domain. *Arch. Biochem. Biophys. 372*, 159–165.
10. Turner, J. H., Gelasco, A. K., and Raymond, J. R. (2004) Calmodulin interacts with the third intracellular loop of the serotonin 5-HT (sub1A) receptor at two distinct sites. *J. Biol. Chem. 279*, 17027–17037.
11. Wang, D. X., Sadée, W., and Quillan, J. M. (1999) Calmodulin Binding to G Protein-coupling Domain of Opioid Receptors. *J. Biol. Chem. 274*, 22081–22088.
12. Cohen, P., and Klee, C. B. (1988) *Calmodulin*, Elsevier, Amsterdam, The Netherlands.
13. Vetter, S. W., and Leclerc, E. (2003) Novel aspects of calmodulin target recognition and activation. *Eur. J. Biochem. 270*, 404–414.
14. Kincaid, R. L., Nightingale, M. S., and Martin, B. M. (1988) *Proc. Natl. Acad. Sci. U.S.A. 85* 8923–8987.
15. Kemp, B. E., Pearson, R. B., Guerriero, V., Jr., Bagchi, I. C., and Means, A. R. (1987) The calmodulin binding domain of chicken smooth muscle myosin light chain kinase contains a pseudosubstrate sequence. *J. Biol. Chem. 262*, 2542–2548.
16. Kennelly, P. J., Edelman, A. M., Blumenthal, D. K., and Krebs, E. G. (1987) Rabbit skeletal muscle myosin light chain kinase. The calmodulin binding domain as a potential active site-directed inhibitory domain. *J. Biol. Chem. 262*, 11958–11963.
17. Colbran, R. J., Schworer, C. M., Hashimoto, Y., Fong, Y. L., Rich, D. P., Smith, M. K., and Soderling, T. R. (1989) Calcium/calmodulin-dependent protein kinase II. *Biochem. J. 258*, 313–325.
18. Wei, Q., and Lee, E. Y. C. (1997) Expression and reconstitution of calcineurin A and B subunits. *Biochem. Mol. Biol. Int. 41*, 169–177.
19. Yang, S. J., Zhang, L., and Wei, Q. (2000) Activities and properties of calcineurin catalytic domain. *Chin. Sci. Bull. 45*, 1394–1398.
20. Xiang, B. Q., Liu, P., Jiang, G. H., Zou, K., Yi, F., Yang, S. J., and Wei, Q. (2003) The catalytically active domain in the A subunit of calcineurin. *Biol. Chem. 384*, 1429–1434.
21. Wang, H. L., Du, Y. W., Xiang, B. Q., Lin, W. L., and Wei, Q. (2007) The regulatory domains of CNA have different effects on the inhibition of CN activity by FK506 and CsA. *IUBMB Life 59*, 388–393.
22. Bradford, M. M. (1976) A rapid and sensitive method for the quantification of microgram quantities of protein utilizing the principle of protein-dye binding. *Anal. Biochem. 72*, 248–254.
23. Ye, Q. L., Li, X., Wong, A., Wei, Q., and Jia, Z. C. (2006) Structure of Calmodulin Bound to a Calcineurin Peptide: A New Way of Making an Old Binding Mode. *Biochemistry 45*, 738–745.
24. Ye, Q. L., Wang, H. L., Wong, A., Li, X., Wei, Q., and Jia, Z. C. (2007) Crystallization Characteristics of Calmodulin in Complex and Fused with Calcineurin Peptide. *Cryst. Growth Des. 11*, 2198–2201.
25. Klee, C. B., Ren, H., and Wang, X. (1998) Regulation of the calmodulin-stimulated protein phosphatase, calcineurin. *J. Biol. Chem. 273*, 13367–13370.
26. Huai, Q., Kim, H. Y., Liu, Y. D., Zhao, Y. D., Mondragon, A., Liu, J. O., and Ke, H. M. (2002) Crystal structure of calcineurin-cyclophilin-cyclosporin shows common but distinct recognition of immunophilin-drug complexes. *Proc. Natl. Acad. Sci. U.S.A. 99*, 12037–12042.
27. Ke, H. M., and Huai, Q. (2003) Structures of calcineurin and its complexes with immunophilins–immunosuppressants. *Biochem. Biophys. Res. Commun. 311*, 1095–1102.
28. Husi, H., Luyten, M. A., and Zurini, M. G. M. (1994) Mapping of the Immunophilin-Immunosuppressant Site of Interaction on Calcineurin. *J. Biol. Chem. 269*, 14199–14204.
29. Kawamura, A., and Su, M. S. S. (1995) Interaction of FKBP12-FK506 with Calcineurin A at the B subunit-binding Domain. *J. Biol. Chem. 270*, 15463–15466.
30. Griffith, J. P., Kim, J. L., Kim, E. E., Sintchak, M. D., Thomson, J. A., Fitzgibbon, M. J., Fleming, M. A., Caron, P. R., Hsiao, K., and Navia, M. A. (1995) X-ray structure of calcineurin inhibited by the immunophilin-immunosuppressant FKBP12-FK506 complex. *Cell 82*, 507–522.
31. Jin, L., and Harrison, S. C. (2002) Crystal structure of human calcineurin complexed with cyclosporin A and human cyclophilin. *Proc. Natl. Acad. Sci. U.S.A. 99*, 13522–13526.

BI702539E